A&A 552, L6 (2013)
DOI: 10.1051/0004-6361/201321380

Astronomy & Astrophysics

Letter to the Editor

A massive parsec-scale dust ring nebula around the yellow hypergiant Hen 3-1379

D. Hutsemékers[1,⋆], N. L. J. Cox[2], and C. Vamvatira-Nakou[1]

[1] Institut d'Astrophysique et de Géophysique, Université de Liège, Allée du 6 août 17, B5c, 4000 Liège, Belgium
e-mail: hutsemekers@astro.ulg.ac.be
[2] Instituut voor Sterrenkunde, KU Leuven, Celestijnenlaan 200D, 3001 Leuven, Belgium

Received 28 February 2013 / Accepted 15 March 2013

ABSTRACT

On the basis of far-infrared images obtained by the *Herschel* Space Observatory, we report the discovery of a large and massive dust shell around the yellow hypergiant Hen 3-1379. The nebula appears as a detached ring of 1 pc diameter which contains 0.17 $M_\odot$ of dust. We estimate the total gas mass to be 7 $M_\odot$, ejected some 1.6×10^4 years ago. The ring nebula is very similar to nebulae found around luminous blue variables (LBVs) except it is not photoionized. We argued that Hen 3-1379 is in a pre-LBV stage, providing direct evidence that massive LBV ring nebulae can be ejected during the red supergiant phase.

Key words. stars: massive – circumstellar matter – stars: mass-loss – stars: individual: Hen 3-1379

1. Introduction

According to current evolutionary models of massive stars (e.g., Maeder & Meynet 2010), O-type stars evolve into Wolf-Rayet stars by losing a significant fraction of their initial mass. Luminous blue variable stars (LBVs) represent a short (a few 10^4 yr) unstable phase in the upper part of the Hertzsprung-Russell (HR) diagram. Their luminosities are typically $5.3 < \log L/L_\odot < 6.3$ and their spectral types between O9 and A (Humphreys & Davidson 1994). LBVs are often surrounded by massive dusty nebulae (Hutsemékers 1994; Nota et al. 1995) which reveal episodes of extreme mass-loss. LBVs likely represent an intermediate stage between main-sequence O-type and Wolf-Rayet stars, for stars with initial mass higher than ~30 $M_\odot$.

It is not clear at which evolutionary stage the massive ($\geq$1 $M_\odot$) nebulae observed around LBVs are ejected, and what is the physical mechanism responsible for their ejection. Based on a dust composition found to be very similar to that of red supergiants (RSGs), Waters et al. (1997) and Voors et al. (2000) argued that LBV nebulae were ejected when the stars were RSGs, although no RSG has been observed with $\log L/L_\odot \geq 5.8$. By comparing the N/O abundances in the ejected nebulae to the predicted surface composition of massive stars during various phases of their evolution, Lamers et al. (2001) concluded that LBV nebulae are ejected during the blue supergiant phase and that the stars have not gone through a RSG phase. But Lamers et al. (2001) only considered a sample of very luminous LBVs, all with $\log L/L_\odot > 5.8$. On the other hand, the determination of C, N, O abundances in the nebula around the less luminous LBV Wray15-751, based on far-infrared spectroscopy with the *Herschel* space observatory, led to the conclusion that the nebula was ejected during a RSG phase (Vamvatira-Nakou et al., in prep.).

Here we report the discovery of a massive parsec-scale dust nebula around the yellow hypergiant Hen 3-1379 which has not yet reached the LBV stage, providing direct evidence for the ejection of LBV-type nebulae during the RSG phase.

⋆ Senior Research Associate F.R.S.-FNRS.

Hen 3-1379 (=IRAS 17163-3907) is an emission-line star discovered by Henize (1976). It has been studied in detail by Le Bertre et al. (1989, 1993). In particular, Hen 3-1379 was found irregularly variable, both photometrically and spectroscopically, with strong infrared emission due to dust, mostly silicate. These authors noticed the strong spectral similarity with the LBV HR CAR, but classified Hen 3-1379 as a post-AGB star due to its low luminosity.

From a detailed study of foreground insterstellar absorption, Lagadec et al. (2011a) revised the distance to Hen 3-1379. They found the star located at ~4 kpc, then with a luminosity $\log L/L_\odot \simeq 5.7$, comparable to that of the LBV Wray15-751, and a late B or early A spectral type, characteristic of yellow hypergiants (YHGs, e.g., Oudmaijer et al. 2009). Mid-infrared imaging (~10 μm) revealed the presence of two concentric dust shells around the star, with radii 0.″6 and 1.″5, indicative of mass-loss enhancement. By modeling the mid- to far-infrared emission, they also predict the existence of a larger and colder dust shell.

2. A large dust nebula around Hen 3-1379

Figures 1 and 2 illustrate the circumstellar environment of Hen 3-1379. A ring nebula is clearly observed in the far-infrared images, with a diameter of approximately 50″.

The observations were carried out with the Photodetector Array Camera and Spectrometer (PACS, Poglitsch et al. 2010) onboard the *Herschel* Space Observatory (Pilbratt et al. 2010), in the framework of the *Herschel* Infrared Galactic Plane survey (Hi-GAL, Molinari et al. 2010). Hi-GAL is a key programme of *Herschel*, mapping the inner part of the Galactic plane at 70 and 160 μm with PACS and 250, 350 and 500 μm with the Spectral and Photometric Imaging Receiver (SPIRE, Griffin et al. 2010). The data are acquired in the PACS/SPIRE parallel mode by moving the satellite at the speed of 60″ s^{-1}. This observing mode results in image elongation along the scan direction. In Hi-GAL two orthogonal scans are secured. This redundancy regularizes the PSF which is roughly symmetric with FWHM of 10″

Fig. 1. A two-color image of Hen 3-1379 and its environment, from *Herschel* PACS observations at 70 μm (blue) and 160 μm (red). The field is 8′× 8′ with a pixel size of 2″. North is up and east to the left. The dust nebula around Hen 3-1379, roughly 50″ in diameter, pops up over the colder interstellar medium.

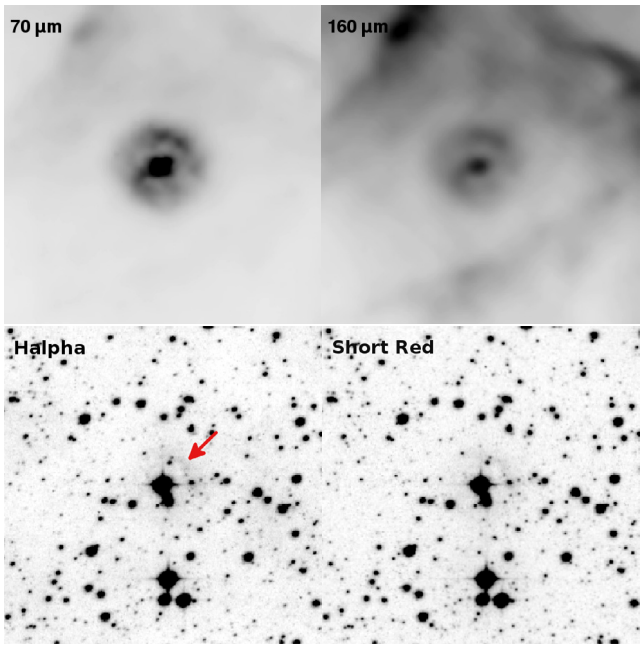

Fig. 2. The 4′× 4′ environment of Hen 3-1379 in the 70 μm and 160 μm *Herschel* PACS bands (*top*), and in the Hα and short red bands of the AAO/UKST SuperCOSMOS Hα survey (*bottom*). North is up and east to the left. The arrow points to a faint reflection arc NW of Hen 3-1379.

and 13″ at 70 and 160 μm respectively (Traficante et al. 2011). The observations, made immediately public for legacy, were retrieved from the *Herschel* archive, pre-processed up to level 1 using the Herschel Interactive Processing Environment (HIPE version 9; Ott 2010), and subsequently reduced and combined using Scanamorphos (version 18; Roussel 2012). Only PACS data were considered, Hen 3-1379 being out of the SPIRE fields.

The dust nebula around Hen 3-1379 appears as a circular, clumpy ring, extending from about 18″ to 40″ around the star with a maximum at roughly 25″. At the distance of 4 kpc, this corresponds to a radius of 0.5 pc, typical of LBV nebulae and identical to the radius of the ring nebula around Wray15-751. The morphology, round and clumpy, is similar to the morphology of the inner "Fried Egg" nebula unveiled by Lagadec et al. (2011a) using the Very Large Telescope Imager and Spectrometer for mid-Infrared (VISIR). On the PACS images, the "Fried Egg" nebula is unresolved and appears as the bright central spot observed at both 70 and 160 μm. The ring nebula is located in a cavity, best seen at 160 μm, 2′−3′ (∼3 pc) in diameter, which delineate a bubble in the ambient interstellar medium, likely blown out by the O star wind in a previous evolutionary phase, although a remnant of an even older phase of mass-loss enhancement cannot be excluded.

Attempts to detect an ionized gas nebula around Hen 3-1379 through Hα imaging failed, either from the ground (Le Bertre et al. 1989) or using the *Hubble* Space Telescope (Siodmiak et al. 2008). In Fig. 2 we show images from the AAO/UKST SuperCOSMOS Hα survey obtained in a narrow-band Hα+[NII] and a broad-band Short Red filter, with bandwidths 6555−6625 Å and 5900−6900 Å respectively (Parker et al. 2005). This survey provides a 5-Rayleigh (i.e., 3×10^{-17} erg cm^{-2} s^{-1} arcsec^{-2}) sensitivity with arcsecond spatial resolution. A faint arc is detected approximately 22″ NW of the star, at a position corresponding to the brightest part of the far-infrared ring. This arc is equally seen in both filters and thus likely due to dust scattering and not to Hα emission. This confirms the absence of ionized gas emission around Hen 3-1379, in particular from the far-infrared dust ring. For comparison, the ionized gas nebula around Wray15-751 (Hutsemékers & Van Drom 1991) is well detected on the images of the SuperCOSMOS Hα survey.

3. Spectral energy distribution and nebular mass

From the PACS images we measure the flux densities F_ν = 386 ± 3 Jy at 70 μm and 55 ± 3 Jy at 160 μm for the whole nebula, using a 80″ aperture and after subtraction of the background emission estimated in the surrounding cavity. The contribution of the unresolved central source is 50 ± 2 Jy at 70 μm and 4.8 ± 0.5 Jy at 160 μm using a 12″ aperture. In this case, we consider both the surrounding cavity and the ring itself to estimate the background emission, the difference being accounted for in the error budget. To account for the small aperture, the flux measured at 70 μm has been increased by 10% and the flux measured at 160 μm by 25% (Ibar et al. 2010; we conservatively assume that the correction at 70 μm is of the order of correction at 100 μm).

To build the spectral energy distribution (SED), we use the ground-based near- and mid-infrared photometric measurements of Le Bertre et al. (1989) and Lagadec et al. (2011b). These data only refer to the star and the inner "Fried Egg" nebula. Other measurements were retrieved from the NASA/IPAC Infrared Science Archive. Only good quality data are used. We consider the IRAS flux densities at 12, 25, and 60 μm, the AKARI FIS measurements at 65 and 90 μm, and the MSXC6 data at 4.29, 4.35, 8.3, 12, 15, and 21 μm. The beam size of the IRAS and AKARI observations is too large to resolve the different dust shells so that these measurements refer to the whole nebula.

All these data are plotted in Figs. 3 and 4. They agree within the uncertainties and variability limits. No color-correction has been applied, because it is small (most often <10%) and difficult to evaluate given the complex SED and the presence of strong

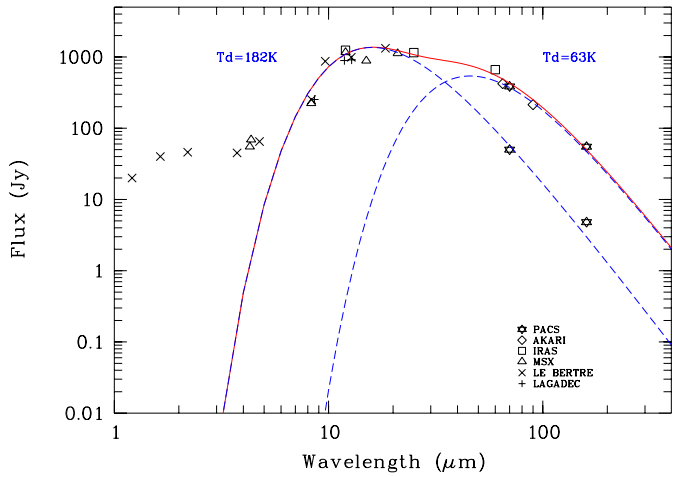

Fig. 3. Spectral energy distribution of Hen 3-1379. The different symbols indicate photometric measurements from various sources. Error bars are not showed for clarity but they are usually comparable to the symbol size. At 70 μm and 160 μm, the two measurements refer to the inner unresolved nebula and to the larger ring, both well separated on the PACS images. The SED is fitted with the sum (red continuous curve) of two modified black-body curves with dust temperatures T_d = 182 K and T_d = 63 K (dashed blue curves).

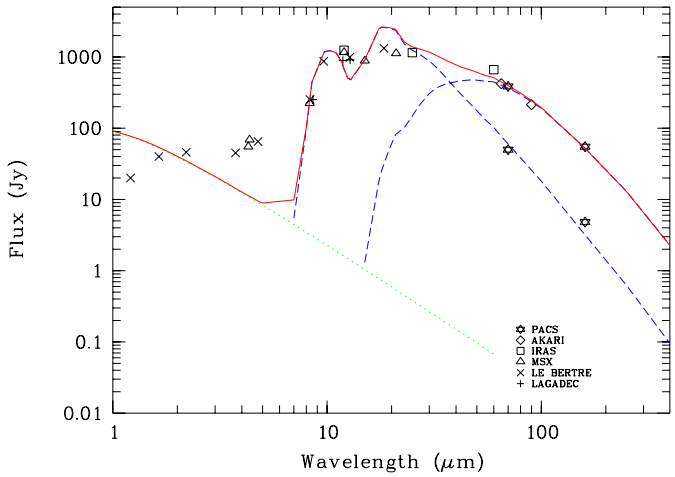

Fig. 4. Same as Fig. 3, but the spectral energy distribution is fitted with the results of the 2-Dust radiative transfer code. The total emission spectrum (red continuous curve) is shown as well as the individual contributions of the inner "Fried Egg" nebula and the outer ring (dashed blue curves). The stellar spectrum is also shown (dotted green line).

silicate emission reported by Le Bertre et al. (1989) on the basis of IRAS low resolution spectra.

The total emission can be fitted as the sum of two modified black-body curves $F_\nu \propto \nu^\beta B_\nu(T_d)$. Since silicates are clearly detected in the nebula around Hen 3-1379 (Le Bertre et al. 1989), we adopt $\beta = 2$. The contributions of the inner "Fried Egg" nebula with a dust temperature T_d = 182 K and the larger ring nebula with T_d = 63 K are clearly separated.

To further model the dust emission we use the two-dimensional radiative transfer code 2-Dust (Ueta & Meixner 2003). 2-Dust is a versatile code which can be supplied with various grain size distributions and optical properties as well as complex density distributions. For 2-Dust, the inner radius of the dust shell is an observable that can be measured from images so that the dust temperature at that radius can be readily computed.

We assume that the nebula around Hen 3-1379 is spherically symmetric, which is a good approximation of the overall geometry, and formed of two separate shells, the first one being the "Fried Egg" nebula imaged by Lagadec et al. (2011a), with r_{in} = 0.″45 and r_{out} = 2.″25, and the second one the large ring seen on the PACS images, with r_{in} = 21.″5 and r_{out} = 40″. In the latter case, the exact value of r_{in} was determined by comparing the PACS images to synthetic ones produced by 2-Dust and convolved with the PSF. In each shell we assume that the dust density runs as r^{-2}. The addition of a third shell to better account for the structure of the "Fried Egg" nebula appeared as an unnecessary complication, only increasing the parameter space. For the stellar parameters, we use the luminosity $\log L/L_\odot = 5.7$, the effective temperature T_{eff} = 8500 K, and the distance d = 4 kpc (Lagadec et al. 2011a). Since the dust in Hen 3-1379 is dominated by silicates, we adopt a composition similar to the one used for modeling Wray15-751 and other LBVs (Voors et al. 2000; Vamvatira-Nakou et al., in prep.), i.e., pyroxenes with a 50/50 Fe to Mg abundance (bulk density 3.2 g cm^{-3}). The optical constants are taken from Dorschner et al. (1995) and extrapolated to a constant refraction index in the far-ultraviolet. We assume a MRN size distribution for the dust grains (Mathis et al. 1977): $n(a) \propto a^{-3.5}$ with $a_{min} < a < a_{max}$, a denoting the grain radius. We did not attempt to fit the 5 μm emission which is likely due to transiently heated dust grains and/or hot dust very close to the star. Adjustment to the data is mostly done by tuning the optical depth, which controls the strength of the emission, a_{max} which controls the 20 μm/100 μm flux ratio in the hotter shell, and the density ratio between the two shells. The two shells were considered simultaneously to reproduce the total energy distribution as well as separately to measure their individual contributions. A good fit is obtained (Fig. 4) except for the 18 μm/10 μm silicate emission band ratio which is too high in the model, without incidence on our results. Acceptable values of a_{max} are found in the 1−3 μm range, indicating the presence of large dust grains around Hen 3-1379 as in LBV nebulae (Voors et al. 2000).

Although there is some degeneracy in the parameter space, the derived dust temperatures and masses are reasonably robust. From the 2-Dust modeling, the temperature of the "Fried Egg" nebula is between 280 and 130 K, in agreement with Lagadec et al. (2011a). For the outer ring, the temperature is between 64 and 52 K. The dust mass is $M_d = 2.1 \times 10^{-3}\ M_\odot$ for the "Fried Egg" nebula and M_d = 0.17 $M_\odot$ for the large ring. Considering other acceptable models, we estimate the uncertainty of the mass to be around 20−30%. M_d can also be derived empirically using $M_d = F_\nu\, d^2\, B_\nu^{-1}\, K_\nu^{-1}$ where K_ν is the mass absorption coefficient roughly independent of the grain radius (Hildebrand 1983). For the silicates of Dorschner et al. (1995), $K_\nu \simeq 49$ cm^2 g^{-1} at 70 μm. With T_d = 182 K, we find $M_d = 1.4 \times 10^{-3}\ M_\odot$ for the "Fried Egg" nebula, and M_d = 0.12 $M_\odot$ for the larger ring nebula with T_d = 63 K, in agreement with the 2-Dust results.

4. Hen 3-1379: a pre-LBV?

In Table 1 we compare Hen 3-1379 to Wray15-751. The latter star is a low-luminosity LBV surrounded by two massive dusty shells likely ejected during a previous RSG phase as revealed by the C,N,O abundances and in agreement with the evolutionary models of a star of initial mass ∼40 $M_\odot$ with little rotation (Vamvatira-Nakou et al., in prep.). The two objects and their ejecta appear very similar. In particular the outer ring nebula associated to Hen 3-1379 has all the characteristics of a bona-fide LBV ring nebula, except it is not photoionized.

Since LBV variations in the HR diagram are only reported when observers catch them, one could imagine that Hen 3-1379 is a true LBV in its cool phase, as supported by the similarity

Table 1. Comparison of Wray15-751 and Hen 3-1379.

	Wray15-751	Hen 3-1379
$\log L/L_\odot$	5.7 ± 0.2	5.7 ± 0.1
$T_{\rm eff}$ (10^3 K)	30 ↔ 9	8.5 ± 1.0
d (kpc)	6.0 ± 1.0	4.0 ± 0.5
r (inner shell) (pc)	0.5	0.04
r (outer shell) (pc)	2.0	0.5
$v_{\rm exp}$ (km s^{-1})	26	∼30
$t_{\rm kin}$ (inner shell) (10^4 yr)	1.9	0.13
$t_{\rm kin}$ (outer shell) (10^4 yr)	7.5	1.6
$M_{\rm d}$ (inner shell) (10^{-2} $M_\odot$)	4.5 ± 0.5	0.21 ± 0.06
$M_{\rm d}$ (outer shell) (10^{-2} $M_\odot$)	5.0 ± 2.0	17 ± 5

Notes. The expansion velocity of the Hen 3-1379 nebula is assumed similar to the one measured for the shell around yellow hypergiant IRC+10420, i.e., $v_{\rm exp} \simeq 25{-}37$ km s^{-1} (Castro-Carrizo et al. 2007). The inner shell of Hen 3-1379 refers to the whole "Fried Egg" nebula and the outer shell to the large ring nebula.

References. Sterken et al. (2008); Vamvatira-Nakou et al. (in prep.); Lagadec et al. (2011a); this work.

of its spectrum to the 1992 spectrum of HR Car (Le Bertre et al. 1993), i.e., when HR Car was itself in a cool phase (van Genderen et al. 1997). However Hen 3-1379 has most probably not (yet) moved blueward. Indeed if the star had been as hot as Wray15-751, it would have similarly photoionized the ring nebula, stellar luminosities and nebular radii being comparable. Assuming comparable nebular densities, the ionization/recombination time scale would be a few hundred years (cf. Vamvatira-Nakou et al., in prep.) so that the ring nebula around Hen 3-1379 should be glowing in Hα as the Wray15-751 nebula, which is not the case. Even a few decades spent in a hot phase would result in a detectable Hα nebula (Appendix A).

According to the kinematical age of the nebulae, Hen 3-1379 looks younger than Wray15-751, with the inner shell possibly still in formation. Hen 3-1379 is most likely in a pre-LBV evolutionary stage. The kinematical age of the ring nebula around Hen 3-1379, 1.6×10^4 yr, indicates that the star has already spend a significant fraction of its time as a post-red supergiant star (cf. the models for a 40 $M_\odot$ star by Ekström et al. 2012). This also suggests that the ring nebula should have been ejected close to the beginning of the RSG phase, possibly due to the dynamical instability mechanism proposed by Stothers and Chin (1996). If we adopt a gas to dust ratio of 40 as measured for the Wray15-751 nebula (Vamvatira-Nakou et al., in prep.), Hen 3-1379 has lost ∼7 $M_\odot$ of gas and dust since the beginning of the RSG phase. Interestingly enough, Wray15-751 has ejected two shells of comparable mass, while for Hen 3-1379, most of the mass is concentrated in the outer ring.

5. Conclusions

We have found a large dust ring nebula around the yellow hypergiant Hen 3-1379. With 1 pc in diameter and a total gas mass estimated to 7 $M_\odot$, this nebula is comparable to the nebulae observed around LBVs. In particular, Hen 3-1379 appears very similar to the low-luminosity (loL; $\log L/L_\odot \lesssim 5.8$) LBV Wray15-751. The fact that the nebula is not seen in Hα indicates that Hen 3-1379 has not yet moved to a hotter phase, and is still in a pre-LBV stage. Hen 3-1379 might be just ready to cross the yellow void and become a hot LBV, a scenario also suggested for IRC+10420 (Humphreys et al. 2002). Our observations strongly support the evolutionary path: RSG → YHG → loL-LBV, providing direct evidence that massive LBV nebulae can be ejected during the RSG phase.

Acknowledgements. D.H., N.L.J.C. and C.V.N. acknowledge support from the Belgian Federal Science Policy Office via the PRODEX Programme of ESA. PACS has been developed by a consortium of institutes led by MPE (Germany) and including UVIE (Austria); KU Leuven, CSL, IMEC (Belgium); CEA, LAM (France); MPIA (Germany); INAF-IFSI/OAA/OAP/OAT, LENS, SISSA (Italy); IAC (Spain). This development has been supported by the funding agencies BMVIT (Austria), ESA-PRODEX (Belgium), CEA/CNES (France), DLR (Germany), ASI/INAF (Italy), and CICYT/MCYT (Spain). This research has made use of the NASA/IPAC Infrared Science Archive, which is operated by the Jet Propulsion Laboratory, California Institute of Technology.

Appendix A: Detection limit of the nebula in Hα

We can roughly estimate the time needed in the hot phase to produce a detectable Hα nebula. Given its sensitivity (Sect. 2), the SuperCOSMOS survey can detect $F(\mathrm{H}\alpha) > 6 \times 10^{-14}$ erg cm^{-2} s^{-1} from a (homogeneous) ionized nebula 25″ in radius. Within a time t, a star emitting Q_0 ionizing photon s^{-1} ionizes $Q_0\,t$ hydrogen atoms. The ionized gas will recombine and emits $F(\mathrm{H}\alpha) = (1/4\pi)\,n_{\rm e}\,n_{\rm p}\,h\nu\,\alpha^{\rm eff}_{\mathrm{H}\alpha}\,V\,d^{-2}$ where $n_{\rm e}$ and $n_{\rm p}$ are the electron and proton densities, $\alpha^{\rm eff}_{\mathrm{H}\alpha}$ the effective recombination coefficient, ν the frequency of Hα, h the Planck constant, V the emitting volume and d the distance to the nebula. Making $n_{\rm e}\,n_{\rm p} = (Q_0\,t/V)^2$ we can estimate the time that the star must emit Q_0 ionizing photon s^{-1} to make its surrounding nebula glowing in Hα above the detection limit of the SuperCOSMOS survey. With $Q_0 = 10^{47}$ photon s^{-1} as found for Wray15-751 (Vamvatira-Nakou et al., in prep.), we find $t \sim 20$ years.

References

Castro-Carrizo, A., Quintana-Lacaci, G., Bujarrabal, V., Neri, R., & Alcolea, J. 2007, A&A, 465, 457
Dorschner, J., Begemann, B., Henning, T., Jaeger, C., & Mutschke, H. 1995, A&A, 300, 503
Ekström, S., Georgy, C., Eggenberger, P., et al. 2012, A&A, 537, A146
Griffin, M. J., Abergel, A., Abreu, A., et al. 2010, A&A, 518, L3
Henize, K. G. 1976, ApJS, 30, 491
Hildebrand, R. H. 1983, QJRAS, 24, 267
Humphreys, R. M., & Davidson, K. 1994, PASP, 106, 1025
Humphreys, R. M., & Davidson, K., & Smith, N. 2002, ApJ, 124, 1026
Hutsemékers, D. 1994, A&A, 281, L81
Hutsemékers, D., & Van Drom, E. 1991, A&A, 251, 620
Ibar, E., Ivison, R. J., Cava, A., et al. 2010, MNRAS, 409, 38
Lagadec, E., Zijlstra, A. A., Oudmaijer, R. D., et al. 2011a, A&A, 534, L10
Lagadec, E., Verhoelst, T., Mekarnia, D., et al. 2011b, MNRAS, 417, 32
Lamers, H. J. G. L. M., Nota, A., Panagia, N., Smith, L. J., & Langer, N. 2001, ApJ, 551, 764
Le Bertre, T., & Lequeux, J. 1993, A&A, 274, 909
Le Bertre, T., Epchtein, N., Gouiffes, C., Heydari-Malayeri, M., & Perrier, C. 1989, A&A, 225, 417
Maeder, A., & Meynet, G. 2010, NewAR, 54, 32
Mathis, J. S., Rumpl, W., & Nordsieck, K. H. 1977, ApJ, 217, 425
Molinari, S., Swinyard, B., Bally, J., et al. 2010, PASP, 122, 314
Nota, A., Livio, M., Clampin, M., & Schulte-Ladbeck, R. 1995, ApJ, 448, 788
Ott, S. 2010, ASP Conf. Ser., 434, 139
Oudmaijer, R. D., Davies, B., de Wit, W.-J., & Patel, M. 2009, ASP Conf. Ser., 412, 17
Parker, Q. A., Phillipps, S., Pierce, M. J., et al. 2005, MNRAS, 362, 689
Pilbratt, G. L., Riedinger, J. R., Passvogel, T., et al. 2010, A&A, 518, L1
Poglitsch, A., Waelkens, C., Geis, N., et al. 2010, A&A, 518, L2
Roussel, H. 2012 [arXiv:1205.2576]
Siodmiak, N., Meixner, M., Ueta, T., et al. 2008, ApJ, 677, 382
Sterken, C., van Genderen, A. M., Plummer, A., & Jones, A. F. 2008, A&A, 484, 463
Stothers, R. B., & Chin, C.-W. 1996, ApJ, 468, 842
Traficante, A., Calzoletti, L., Veneziani, M., et al. 2011, MNRAS, 416, 2932
Ueta, T., & Meixner, M. 2003, ApJ, 586, 1338
van Genderen, A. M., de Groot, M., & Sterken, C. 1997, A&AS, 124, 51
Voors, R. H. M., Waters, L. B. F. M. , de Koter, A., et al. 2000, A&A, 356, 501
Waters, L. B. F. M., Morris, P. W., Voors, R. H. M., & Lamers, H. J. G. L. M. 1997, ASP Conf. Ser., 120, 326